13th International Brick and
Block Masonry Conference
Amsterdam, July 4-7, 2004

EXPERIMENTAL AND NUMERICAL INVESTIGATIONS ON THE BEHAVIOUR OF UNREINFORCED MASONRY BUILDINGS UNDER SEISMIC LOADINGS

D. Schermer[1]

Abstract

To investigate the behaviour of unreinforced masonry constructions under seismic loadings pseudo-dynamic full-scale tests have been carried out on a plane 3-DOF system. The stiffness characteristics of the upper 2 stories were considered during the tests just numerically by a sub-structure meanwhile the wall of the first storey was tested under combined vertical and horizontal loadings. The nonlinear characteristics of the sub-structure were determined in preceding static-cyclic test under adapted normal forces. In addition to the experiments a non-linear material model has been developed and adopted in a finite-element-programme. The conclusion can be drawn that unreinforced masonry structures showed a significantly better behaviour under seismic loadings than determined in current codes with a behaviour factor of q=1.5.

Key Words

Earthquake, pseudo-dynamic, sub-structure, material model.

1 Introduction

According to the current European Earthquake Standard Eurocode 8 seismic loads increase significantly in regions of low seismicity, e.g. Central Europe. Combined with the proposed behaviour factor q=1.5 the earthquake resistance of several common types of unreinforced masonry buildings can't be proven longer numerically.
To investigate the seismic behaviour of unreinforced masonry constructions under realistic conditions, tests on full scale masonry walls were necessary. Within these experiments the load bearing capacity under combined shear and normal stress and also the load-deformation behaviour were tested.
The chosen pseudo-dynamic test method allowed considering the characteristics of regions of low seismicity, e.g. the earthquake duration and the frequency range of the seismic input resp. the response spectra.

[1] Detleff Schermer, Dipl.-Ing., Head of the Masonry Research Group at the Institute of Concrete and Masonry Structures, Technical University Munich, Germany, schermer@fam-schermer.de.

2 Investigated structure

The investigated masonry structures are composed of concrete slabs – distributing the horizontal loads – and vertical masonry walls. The vertical and also the horizontal loads are carried by the unreinforced masonry shear-walls (s. figure 1).

2.1 Used Materials

For the tested walls the following materials were used (1st and 2nd series).

Table 1 Materials of the tested walls

Wall [1)]	Material	Unit dimensions	Mortar
A, B, C, D	vertically perforated lightweight clay bricks f_b=12N/mm² 	495 mm × 175 mm × 238 mm	cement-lime mortar
E, F	vertically perforated lightweight clay bricks f_b = 12N/mm² 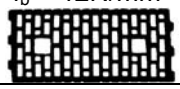	378 mm × 175 mm × 247 mm	thin-layer mortar (wall E) cement-lime mortar (wall F)
KS1, KS2	sand-lime blocks – f_b=20 N/mm² 	998 mm × 175 mm × 498 mm	thin-layer mortar
KS3, KS4	sand-lime bricks – f_b=20 N/mm² 	499 mm × 175 mm × 248 mm	thin-layer mortar with different adhesive shear strength
[1)] Walls A, B and C tested in the first series			

Table 2 Survey of the tested walls

Wall	Execution	Wall dimensions	Perpend joints
A, B, C, D	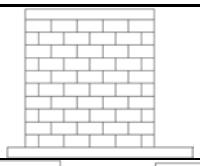	250 cm × 250 cm × 17,5 cm	unfilled
E, F[1)]	E: 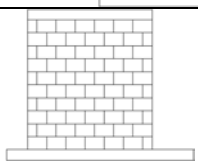 F: 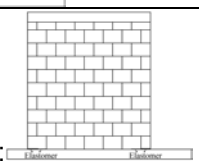	243 cm × 250 cm × 17,5 cm	unfilled
KS1, KS2	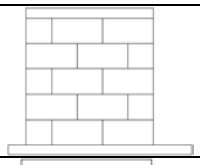	250 cm × 250 cm × 17,5 cm	unfilled (wall KS1) resp. filled (wall KS2)
KS3, KS4	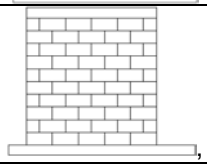	250 cm × 250 cm × 17,5 cm	unfilled
[1)] Wall F with elastomer plates 200 mm × 175 mm × 8 mm & 200 mm × 175 mm × 5 mm in the bottom corners	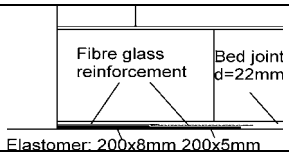		

2.2 Reduction and sub-structure

The investigated 3-storey terraced house was reduced to a plane multi-degree-of-freedom system with elastic restraint in the concrete slabs.

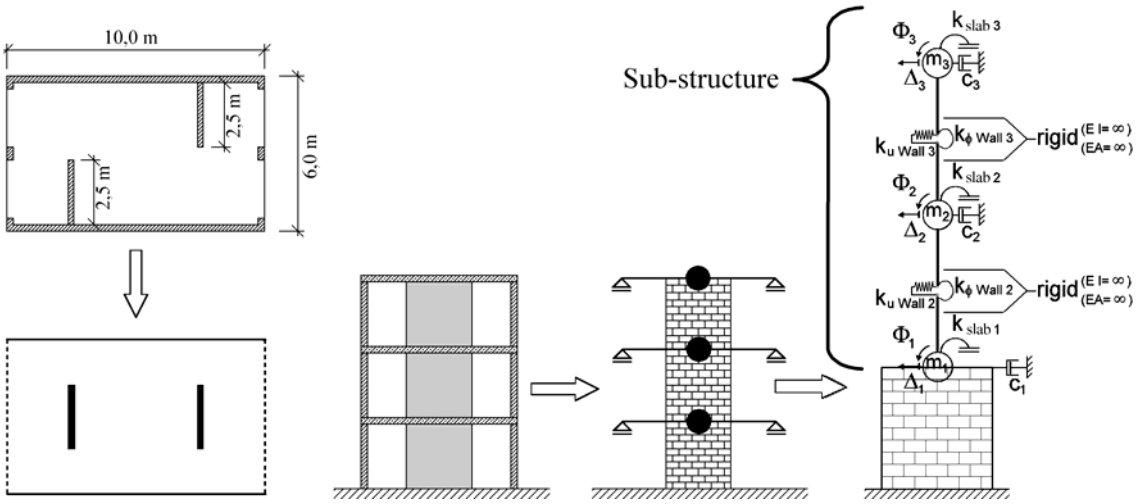

Figure 1 Reduction of the structure to a plane multi-degree-of-freedom system and substitution of the upper two stories of the structure by a sub-structure

The tests were carried out just on the relevant shear wall in the first storey. The upper stories with the shear-walls and their elastic restraint in the concrete slabs were considered numerically as a sub-structure. Its stiffness characteristics in the shape of nonlinear springs were determined within preceding static-cyclic tests under adapted normal forces.

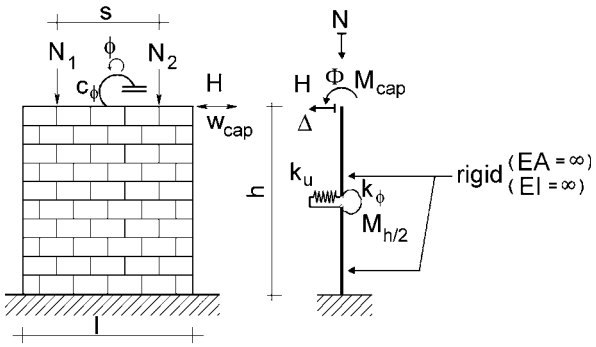

Figure 2 System of the preceding tests and substitution by non-linear shear- and bending-springs

Within these preceding tests the normal force $N = N_1 + N_2$ was varied in the expected range in the 3 storeys, i.e. in levels of 90, 180 and 270kN. The tests were carried out under static-cyclic horizontal loads H. Adapting the boundary conditions of real structures, the appearing cap rotation ϕ resp. Φ was restricted by the application of a bending spring $c_\phi = M_{cap} / \phi$ at the cap of the wall. Its stiffness within these preceding tests was also varied in a wide range of 0 ($M_{cap} = 0$) $\div \infty$ ($c_\phi = 0$) to cover all possible states in the sub-structure. The bending moment at the cap of the wall $M_{cap} = (N_1 - N_2) \times s/2$ was applied by different normal forces N_1 and N_2 in the two computer-controlled hydraulic actuators (figure 3).

The evaluation of the collected data led to a description of the stiffnesses k_ϕ and k_u in dependency on the associated relative rotations Φ and relative displacements Δ resp. moment loadings in the middle of the wall $M_{h/2}$ (wall D) (table 3).

Table 3 Stiffness characteristics of the sub-structure

Wall [1]	K_{u2} [2] [kN/mm]	k_{u3} [2] [kN/mm]	$k_{\phi 2}$ [2] [kNm/mrad]	$k_{\phi 3}$ [2] [kNm/mrad]
D	70:$\|M_{h/2}\|$=0kNm 35:$\|M_{h/2}\|$≥45kNm (type 1) [3]	47:$\|M_{h/2}\|$=0kNm 23:$\|M_{h/2}\|$≥80kNm (type 1) [3]	≡ 200	≡ 125
E	≡ 60	≡ 45	≡ 200	130:$\|\Phi\|$=0mrad 60:$\|\Phi\|$≥0,8mrad (type 2) [3]
F	≡ 42	35:$\|\Delta\|$=0mm 25:$\|\Delta\|$≥2mm (type 2) [3]	≡ 80	55:$\|\Phi\|$=0mrad 28:$\|\Phi\|$≥1,5mrad (type 2) [3]
KS1	≡ 220	≡ 120	≡ 320	220:$\|\Phi\|$=0mrad 120:$\|\Phi\|$≥0,4mrad (type 2) [3]
KS2	330:$\|\Delta\|$≤0,1mm 200:$\|\Delta\|$≥0,4mm (type 3) [3]	170:$\|\Delta\|$=0mm 100:$\|\Delta\|$≥0,5mm (type 2) [3]	400:$\|\Phi\|$≤0,1mrad 310:$\|\Phi\|$≥0,2mrad (type 3) [3]	250:$\|\Phi\|$=0mrad 120:$\|\Phi\|$≥0,25mrad (type 2) [3]
KS3; KS4	≡ 260	180:$\|\Delta\|$=0mm 135:$\|\Delta\|$≥0,4mm (type 2) [3]	400:$\|\Phi\|$=0mrad 300:$\|\Phi\|$≥0,23mrad (type 2) [3]	230:$\|\Phi\|$=0mrad 140:$\|\Phi\|$≥0,35mrad (type 2) [3]
Additional information: $m_1=m_2=m_3$=29 t; $h_1=h_2=h_3$=2.6 m; $k_{slab,i}$ =300 kNm/mrad (except: KS1-2 & 1-3: 600)				

[1] walls A, B and C tested in the first series; [2] secant stiffness

[3]

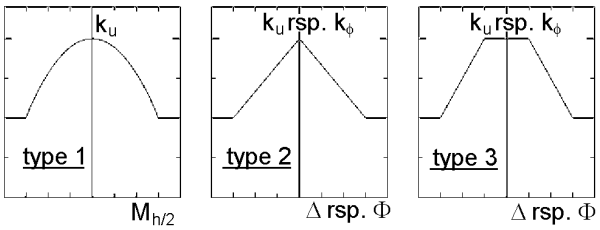

The stiffness of the concrete slabs k_{slab} was determined considering the stiffness reduction by cracks. The total stiffness matrix based on the condensed displacements $\Delta_{1,2,3}$ and rotations $\Phi_{1,2,3}$ of the storey masses.

2.3 Damping

In real structures due to several material and structural effects under dynamic loadings damping can be observed. Generally this can be simple described by viscous dampers. In the investigated systems three single viscous dampers in the level of the storey masses were arranged (s. figure 1). Theirs values $c_{1,2,3}$ were determined according to the target damping rate of 5% of the whole structure.

3 Tests

The tests were carried out at the laboratories of the Institute of Concrete and Masonry Structures at the Technical University Munich (www.mb.bv.tum.de). Detailed results are found in Zilch / Schermer (2002), Schermer (2003) and Zilch / Schermer (2004).
The normal force and the cap moment were applied with two independent computer controlled hydraulic actuators. They were arranged between the roller bearing on top of the concrete cap beam and the horizontal girder of the test frame (detail in figure 2). The horizontal displacements were also applied by a computer-controlled hydraulic actuator with a high accuracy of 4/100 mm. To avoid any unintentional restraint effects, in the middle of the cap beam a moment hinge was arranged.

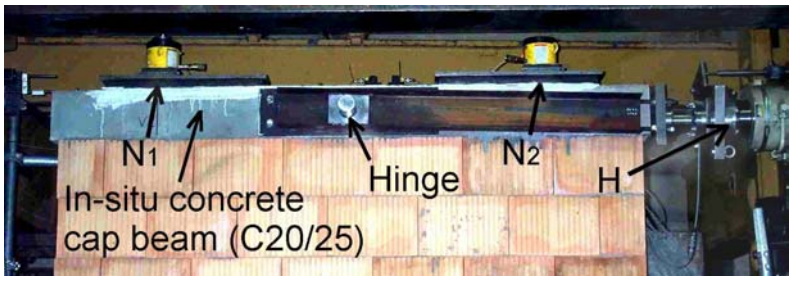

Figure 3 Details of the load application facilities in the test frame (wall E)

3.1 Measurements

During the tests the displacements in all relevant points were measured continuously. Also the horizontal restoring force H and the vertical forces N_1 and N_2 were measured with a frequency of 50 Hz.

3.2 Seismic input

The used artificial ground acceleration time histories were generated adjusted to the elastic response spectra of the new German Earthquake Code DIN 4149 (2002-10) based on Eurocode 8. The total earthquake duration of 9.0 s and the intensity function were adapted to the conditions in regions of low seismicity in Central Europe. The seismic load level was increased stepwise in each test with the load-level factor f (figure 4 and table 4).

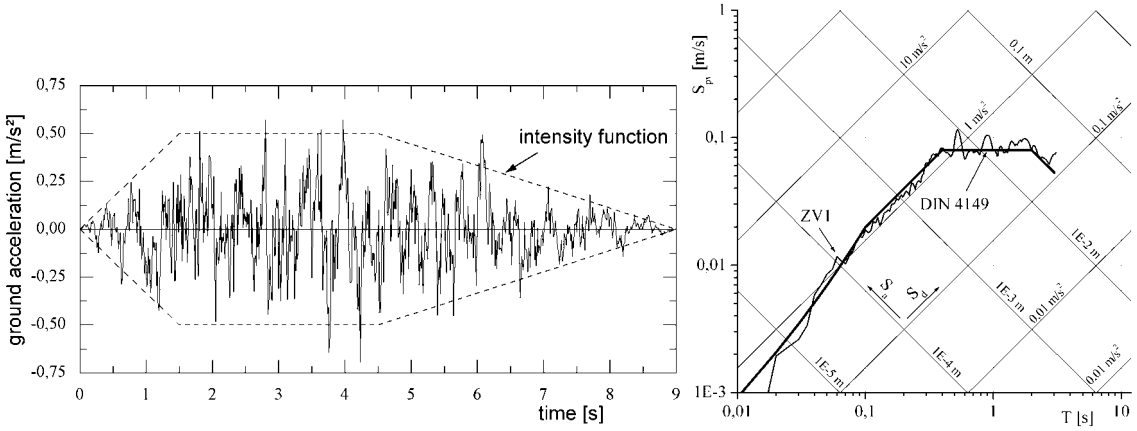

Figure 4 Artificial time history ZV1 with intensity function (a_g=0.4m/², f=1) and corresponding response spectra compared to the task spectra of DIN 4149

3.3 Pseudo-dynamic test-method

For the experimental investigations the pseudo-dynamic test-method was used. The numerical integration of the equation of motion $\underline{m} \cdot \underline{a} + \underline{c} \cdot \underline{v} + \underline{r}(d) = -\underline{m} \cdot \underline{a}_g$ was carried out using the implicit α-method basing on the Newmark method.
As the numerical effort for measurements and controlling was very high, two PCs had to be used. The master computers part was the measurement and controlling of the actuators and also to display the results real-time on a screen. The slave computer carried out the implicit time integration algorithm. For data exchange between the two computers a serial connection-cable was used. Totally each test took about 70 minutes.

4 Results

4.1 Stiffness

The linear-elastic calculation of the horizontal wall-stiffness taking E-modulus from literature resp. design codes led to values much higher than appeared in the tests. The relation was between 1.5 and 3.3 (in the first storey with N = 270kN) and between 3.0 and 5.9 (in the third storey with N = 90kN). In general a high dependency on the normal force resp. the effect of opening bed-joints was found.

For the description of the stiffness and its degradation not only the load-displacement-relation (H-w_{cap}-hysteresis, e.g. figure 10) is important. Also the bending stiffness and the co-action with the horizontal displacements have to be considered. As a consequent, for further investigations the stiffness of the whole structure was calculated from the time-displacement history. The first eigenperiod $T_{1,FFT}$ was determined using the fast-fourier-analysis to the displacement histories in the first storey Δ_1.

For evaluation as reference value $T_{1,elastic}$ calculated on an linear elastic system using the maximum stiffness values under minimal stress (s. table 3) has been taken.

The illustration in figure 5 has been carried out in dependency on the load level, calculated from the relation of maximum appeared horizontal force in the mentioned test and the maximum horizontal force of all test of the investigated wall.

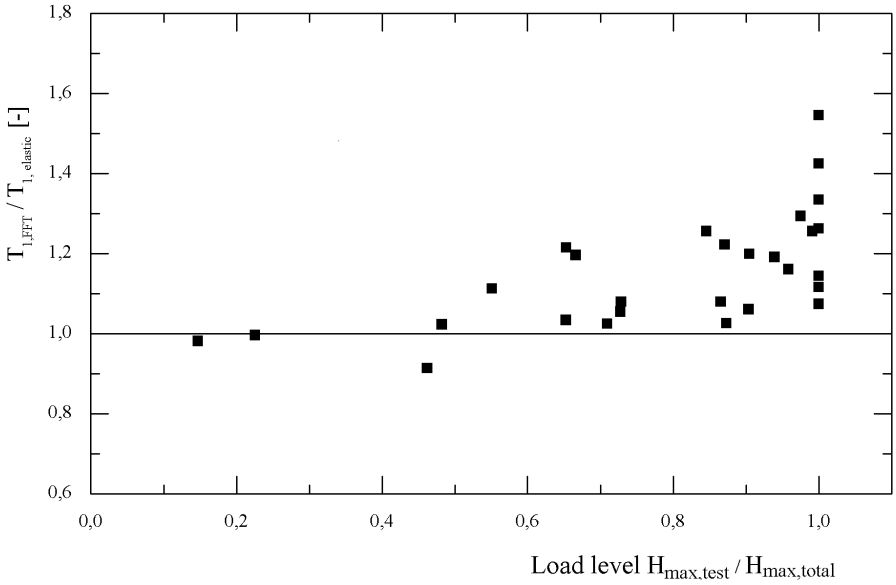

Figure 5 Stiffness reduction versus load level (2nd series)

It was found, that the stiffness degradation at the maximum load level lay between 1.07 and 1.55 (mean value 1.27).

4.2 Load reduction

For seismic design, the under linear-elastic behaviour calculated horizontal loads usually are reduced with the behaviour factor q. It is determined for unreinforced masonry in current codes e.g. Eurocode 8 to q = 1.5.

In the described tests, with the measured initial system-stiffness in a first step a linear calculation of the whole system has been carried out. The resulting theoretical maximum horizontal loads H_{calc} were compared in a second step to the maximum loads appeared in the tests H_{test}. The illustration of this ratio is carried out against the load level, calculated from the ratio of maximum appeared horizontal force in the mentioned test $H_{max,test}$ and the maximum horizontal force of all tests of the investigated wall $H_{max,wall}$. Also in figure 7 the ratio of maximal cap displacement appeared in the tests

$w_{cap,test}$ and the results of a linear-elastic calculation with initial stiffness $w_{cap,calc.}$ is shown.

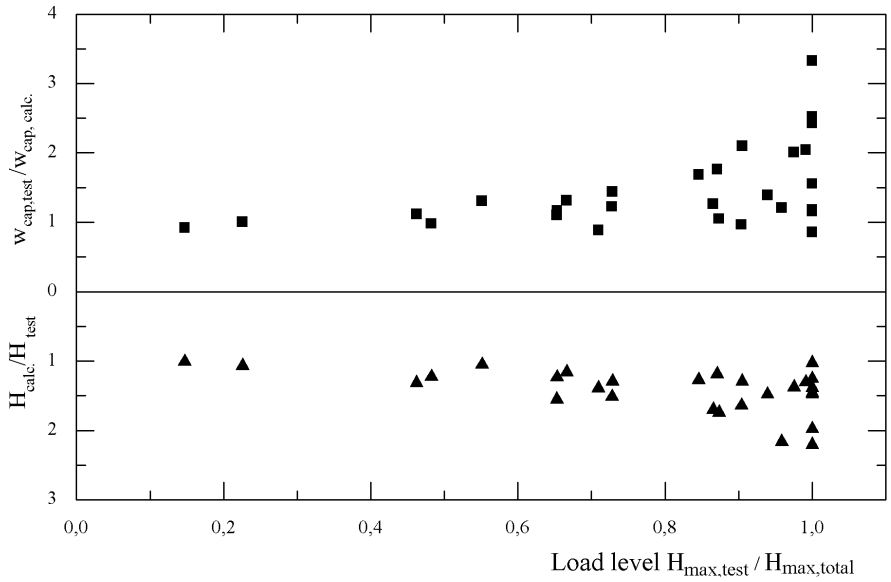

Figure 6 Load reduction and displacement enhancement in the tests versus load level

It is obvious, that with rising load levels the reduction of the calculational horizontal load and the increasing calculational cap displacement grow. The mean value of $H_{calc.}/H_{test}$ is 1.42 (range 1.0 ÷ 2.21) and slightly less than the mean value of $w_{cap,test}/w_{cap,calc.}$ found to 1.46 (range 0.86 ÷ 3.33). At the maximum load level the ration of $H_{calc.}/H_{test}$ ranges from 1.03 (KS2-2) to 2.21 (KS1-7) (mean value 1.54) and the ratio of $w_{cap,test}/w_{cap,calc.}$ ranges from 0.86 (D-4) to 3.3 (KS4-4) (mean value 1.86).

Table 4 Maximum horizontal loads and cap displacements in the tests (extract)

Wall / Test	Time history [1]; Load factor f [-]	Maximum cap displacement w_{cap} [mm]	Maximum horizontal force H [kN]
D-1	ZV1-B3 (a_g=0.4m/s²); f=0.15	0.33	22.8
D-4	f=2	4.11	154.9
D-5	f=2.67	4.52 [2]	145.5 [2]
E-1	ZV4-C3 (a_g=0.4m/s²); f=1	1.5	61.8
E-2	f=2.67	4.27 [2]	112.1 [2]
F-1	ZV3-A1 (a_g=0.4m/s²); f=2	1.85	55.7
F-2	ZV4-C3 (a_g=0.4m/s²);f=3	5.37	115.4
F-3	ZV3-A1 (a_g=0.4m/s²); f=7	8.0 [2]	110.6 [2]
KS1-1	ZV3-A1 (a_g=0.4m/s²); f=2	0.87 [2]	76.6 [2]
KS1-2	f=2	1.18	108.2
KS1-7	f=6	3.36	165.7
KS1-8	f=8	3.21 [2]	149.9 [2]
KS2-1	ZV3-A1 (a_g=0.4m/s²); f=1	0.37	47.3
KS2-2	f=8	3.62 [2]	209.4 [2]
KS3-1	ZV1-B3 (a_g=0.4m/s²); f=1.5	1.26	117.3
KS3-3	f=2.5	3.25	174.5
KS3-4	f=3.5	3.88 [2]	176.0 [2]
KS4-1	ZV1-B3 (a_g=0.4m/s²); f=1.5	1.12	110.6
KS4-3	f=2.5	3.19	165.1
KS4-4	f=3.5	5.42 [2]	169.3 [2]

[1] A/B/C/1/2/3: Soil-subsoil conditions; a_g: ground acceleration; [2] Test stopped premature

5 Numerical investigations

5.1 Failure modes

According to the theory of Mann and Müller (1982) it can be assumed, that in the perpend joints no stresses can be transmitted. Investigating a single brick, the following stress state can be identified:

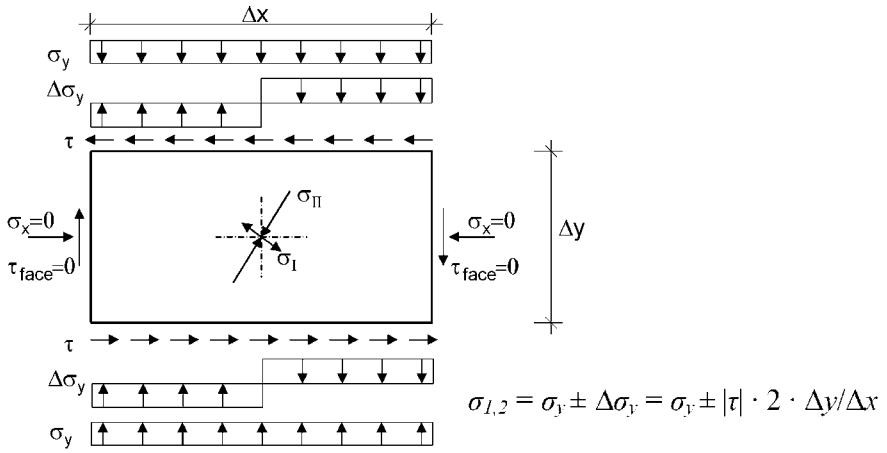

Figure 7 Stress state on a single brick under combined normal- and shear-stresses according DIN 1053-1 and Mann / Müller (1982)

The failure criterions can be classified in

- friction failure in the bed joint $\tau = \mu \times (\sigma_y - \Delta\sigma_y) + k$ (s. figure 7 & 8)
- diagonal tension failure in the brick $\sigma_I = f_{bt}$ (s. figure 7 & 8)
- compression failure $\sigma_1 = \sigma_y + \Delta\sigma_y = f_{my}$
- tension failure in the bed joint $\sigma_2 = \sigma_y - \Delta\sigma_y = f_{ty}$

The material strength parameters were determined in additional material tests (f_{bt} and cohesion k) or calculated using empiric formulas given in literature (f_{my} resp. μ). The deformation parameters used in the material model e.g. E-modulus, were taken from literature.

The observed maximum loads and the failure modes corresponded with the calculated value resp. expected failure modes according Mann/Müller (1982). In the described way, the minimal overlapping length between the bricks of adjacent layers was taken exactly from the existing walls to $0.5 \times \Delta x$ resp. $1.0 \times \Delta y$ (figure 6). Differing, in the design code DIN 1053-1 the overlapping length is set to $0.4 \times \Delta y$. Therefore and because of the very conservative determination of the material strength parameters significant load bearing reserves were identified.

5.2 Material model

In addition to the above described test, a nonlinear material model based on theory of plasticity has been developed. The flow rules were generated from the appearing failure modes according the theory of Mann/Müller (1982), since unreinforced masonry cannot be described by just one simple flow rule. The main advantage of the model is the low number of necessary parameters, mainly determined by standard tests.

Plastic strain in case of friction failure in bed joints was generally not limited, because almost ideal plastic behaviour occurred in tests. Parameters of the linear softening were determined from the fracture energy given in literature. The plastic strain in failure mode tension in the brick has to be transformed to the corresponding shear-deformation. The parameters for linear-softening were also derived from the corresponding fracture energy. The work-hardening rule under compression loadings perpendicularly to the bed joints was taken according to the strain-stress relationship

from standard compression tests and simplified by a combination of a linear and parabolic curve. The unloading runs in parallel to the primary loading curve in the origin.
The verification was carried out on well documented tests. The accordance of maximum loads, occurred failure mode and qualitative load-displacement curves was good.

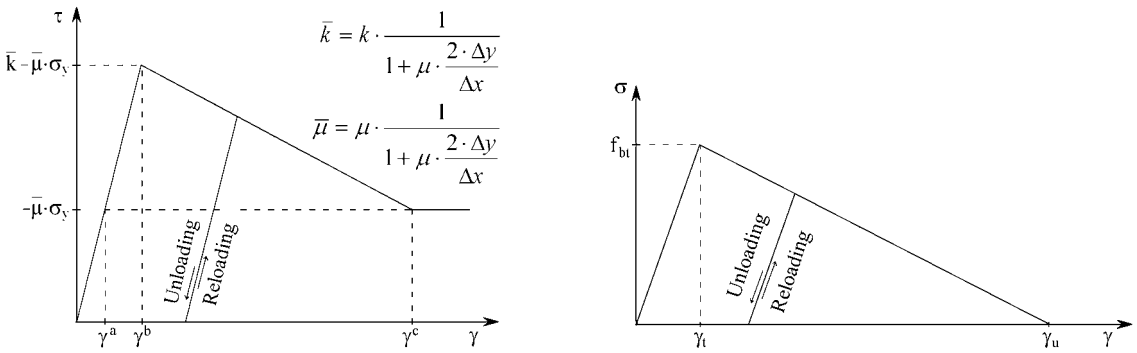

Figure 8 Failure criterion 1 (friction failure in the bed joints) and criterion 2 (diagonal tension failure in the bricks)

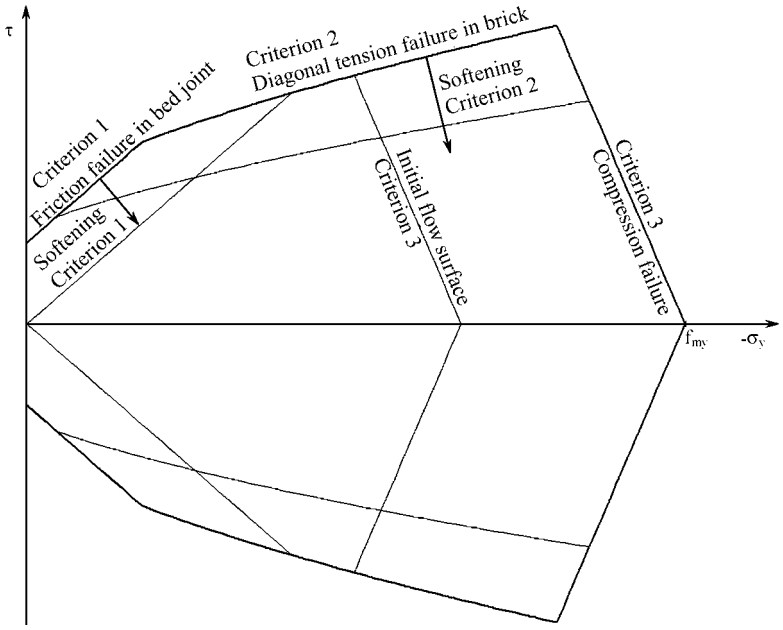

Figure 9 Resulting failure surfaces and flow rules of the material model

Using the deformation parameters, e.g. E-modulus, given in literature leads to stiffness values of the walls much higher than observed in the tests. Reasons can be found in the effects of stiffness reduction due to initial cracking, a different E-modulus at compression perpendicular to the bed joints resp. diagonal under combined shear-/ normal-stresses and the anisotropy of the walls generally due to the bricks itself (e.g. vertically perforated bricks, s. table 1) and the filled or unfilled perpend joints.

5.3 Parametric studies

Using the developed material model, a parametric study was carried out afterwards. Herein the material parameters, the geometric shape of the wall-specimen and the earthquake-load were varied. The tests on a plane finite-element-model were performed dynamically on a simplified SDOF-system (similar to figure 2) under different acceleration time histories. The spacial co-action of the walls and slabs was

considered by an elastic bending spring $c_{\Phi,cap}$ at the cap of the wall coupling cap rotation and cap moment. The dynamic parameters of cap mass and damper were determined for a first eigenperiod of T=0.3s and a damping rate of 5%. The test results were compared to the loads resulting form a linear-elastic calculation. The determination of the load-reduction combined with the nonlinear behaviour of the system led to of behaviour factor values in a range of q=1.4 ÷ 2.0.

5.4 Load-displacement curves

The comparison of calculated and measured load-displacement curves led to a generally good match, although the stiffness of the finite-element-calculation was too high. Exemplary subsequent the results of the test KS4-3 are shown.

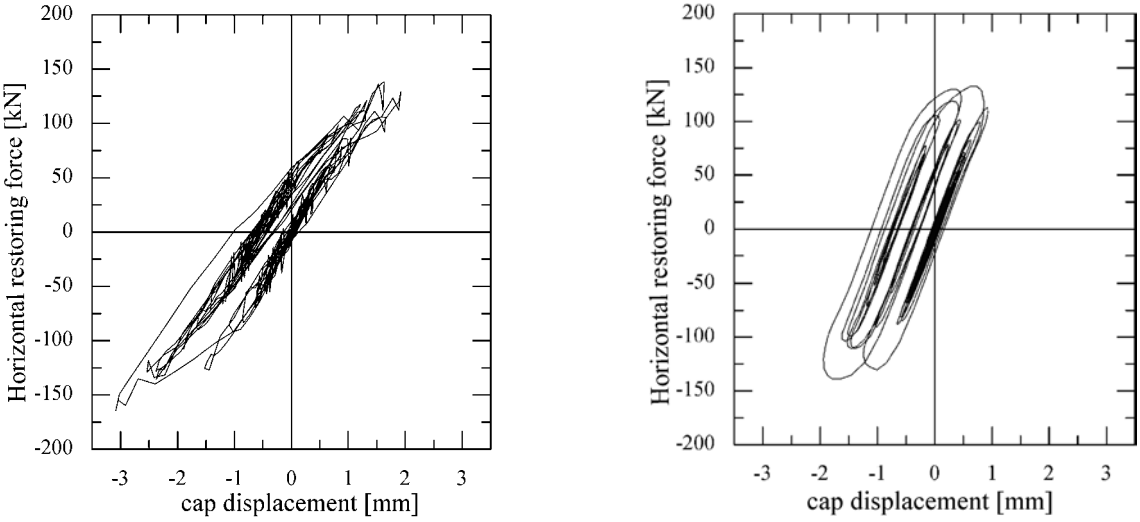

Figure 10 Load-displacement curve of test KS4-3 and corresponding numerical result

6 Conclusions

The described pseudo-dynamic test method with sub-structure technique leads to realistic conditions. As a result of the experimental investigations – confirmed by the numerical investigations and parametric studies – the conclusion can be drawn, that a higher behaviour factor than q = 1.5 is justifiable for URM under the characteristic seismic loads and boundary conditions. Also higher load bearing capacities occurred than expected according to the current design codes. Research in future will focus on wall systems with t-shaped cross section and the optimisation of material properties.

References

Mann, W., Müller, H., 1982: Failure of shear-stressed masonry - an enlarged theory, tests and application to shear walls, Proc. British Ceramic Society, Vol. 30, pp. 223-235 (1982)

Zilch, K.; Schermer, D., 2004: Experimentelle und numerische Untersuchungen zum Erdbebentragverhalten unbewehrter Mauerwerksbauten, In: Schubert (Ed.): Mauerwerk-Kalender 2004, pp. 649-664. Ernst & Sohn, Berlin.

Zilch, K.; Schermer, D.; Scheulfer, W., 2002: Simulated Earthquake behavior of unreinforced masonry walls, In: Grundmann (Ed.): EUORDYN 2002, Munich.

Schermer, D., 2003: Verhalten von unbewehrtem Mauerwerk unter Erdbebenbeanspruchung. Dissertation TU Munich (German language), to be published, 2003.